Mineralogical Magazine, October 2002, Vol. 66(5), pp. 733–744

Mineral physics: the atomic, mesoscopic and macroscopic perspective

E. K. H. SALJE* AND S. RÍOS

University of Cambridge, Department of Earth Sciences, Downing Street, Cambridge CB2 3EQ, UK

ABSTRACT

The macroscopic behaviour of minerals is not always directly related to their crystalline structure at the atomic scale but often depends explicitly on mesoscopic (nanometer–micrometer) features. This paper reviews various cases where the macroscopic phenomena differ from those of the bulk, with structural and chemical variations related to: domain walls, leading to enhanced or reduced transport properties; surfaces controlling growth morphologies; and radiation-damaged minerals where the interface between the amorphous and crystalline phase is believed to play a key role in hydrothermal leaching behaviour. Minerals explicitly discussed are: quartz, agate, hydroxylapatite, cordierite and metamict zircon.

KEYWORDS: mineral physics, mesoscopic features, domain walls, ionic transport, growth morphologies, radiation damage, silica polymorphs, cordierite, zircon.

Introduction

MANY minerals represent complex thermodynamic systems with a multitude of interacting degrees of freedom. The macroscopic description of their response functions, using continuum theories, has been the focus of much research during recent decades. Some of the most potent approaches used Landau-Ginzburg type expressions for non-parabolic thermodynamic potentials (Salje, 1992*a*,*b*; Carpenter *et al.,* 1998*a*; Carpenter and Salje, 1998; Malcherek *et al.,* 1997). These potentials were then coupled with macroscopic observables, such as the spontaneous strain and elastic constants, magnetization and magnetic susceptibilities, spontaneous polarization and dielectric functions etc. (Salje, 1993). The advantage of this approach is that it is based on the formally well-defined thermodynamic limit (number of particles, time $\xrightarrow{\text{limit}}$ infinity) and uses only continuum theory. Despite certain mathematical complexities, the approach was highly successful and led to quantitative expressions of Landau potentials of many important minerals (Carpenter *et al.,* 1998b; Salje 1994; Carpenter and Salje, 1994*a*,*b*; Malcherek *et al.,* 1995; Salje *et al.,* 1998*a*; Hayward and Salje, 1999).

Landau type theory also became the meeting point between experimentalists who could formalize their observations using this theory, phenomenologists, and those who used various levels of computer simulation to build macroscopic systems from atomic wave functions. The latter group made great advances by, for example, introduction of the Siesta-code (Ordejón *et al.*, 1996) that is particularly suitable for the simulation of local phenomena in minerals. This combination of approaches immediately highlighted a number of previously unknown scaling properties. Firstly, effects on local length scales (e.g. as seen in nanocrystals) can be fundamentally different from those of mesoscopic length scales (where surface relaxations and microstructures become important) and those of macroscopic properties (viz. bulk elastic constants do not describe super plasticity that originates from mesoscopic behaviour). Secondly, minerals under geological conditions are often not in thermodynamic equilibrium so that a proper assessment of kinetic theories becomes important. Thirdly, many minerals are heterogeneous on an atomic length scale (e.g. metamict minerals) so that their macroscopic behaviour is often ascribed to

* E-mail: es10002@esc.cam.ac.uk
DOI: 10.1180/0026461026650058

percolation behaviour rather than bulk properties. It is the purpose of this paper to give examples for some of these advances and to relate them to the development of current mineralogical research.

Atomic and mesoscopic processes as the origin of macroscopic features: the case of quartz

The $\alpha-\beta$ transition of quartz is a well-studied phenomenon with a full description of its macroscopic features given by Carpenter *et al.* (1998*b*). Those authors also derived a Landau-Ginzburg potential that reproduces the temperature evolution of lattice parameters and elastic constants at temperatures above room temperature. Quantum behaviour at low temperatures was found for strain data by Pérez-Mato and Salje (2001) with a saturation temperature $\theta_s \approx 190$ K. Despite the almost complete understanding of this transition in the thermodynamic limit, several crucial questions cannot be answered using this approach. One question relates to the nature of the β-phase as a time-averaged structure (how does the structure appear on a time-scale shorter than that needed for the time-average?). Other questions relate to ionic transport (how do ions diffuse in quartz?) and to compact nanoscale quartz (does agate undergo the $\alpha-\beta$ transitions?).

In the next three sections a brief description is given of how the characteristics of β-quartz are related to the simultaneous change of the long/short-range order at the transition, how diffusion is enhanced by the structural features of the twin wall and how in mesoscopically structured nanoquartz boundary conditions affect the character of the α-β transition.

The local structure of β-quartz

What is probably the most advanced molecular dynamics study, by Müser and Binder (2001), shows that SiO_4 tetrahedra are already considerably deformed in the β-phase and do not deform significantly any further at the phase transition. Two relaxation mechanisms were identified, namely the relaxation of the orientation of deformed tetrahedra and relaxation of the oxygen position onto their ideal β-quartz positions. The former relaxation occurs on short time-scales (0.4 ns at $T = T_{tr} + 140$ K) while the latter process is much slower. The orientational relaxations have nothing to do with α_1 and α_2 domains in β-quartz as previously stated by Tsuneyuki *et al.,* (1990). This simple dynamical domain-switching model is also incompatible with the observation of soft modes (Axe and Shirane, 1970; Tezuka *et al.,* 1991) and the absence of symmetry-forbidden phonons in the β-phase (Salje *et al*., 1992). The finding of Müser and Binder (2001) is the existence of slow motion relaxation which implies that the local β-quartz structure does not fluctuate around the ideal β-quartz structure. The oxygen atoms fluctuate around time-dependent equilibrium positions that average to the ideal β-quartz structure only on time-scales longer than 1 ns. A snapshot of the β-quartz structure is shown in Fig. 1. Tucker *et al.* (2000) studied the local and long-range structural order simultaneously by neutron total scattering. Their results agree fully with a concurrent change in the long and short-range structural order during the transition. Thus, as stated by Müser and Binder (2001), "the disorder in β-quartz is unequivocally unrelated to a (hypothetical) coexistence, of finite α_1 and α_2 domains in β-quartz above T_{tr}".

Anisotropic ionic transport in quartz, WO_3 and feldspar

The crystal structure of α-quartz contains wide channels that may be expected to act as fast diffusion paths for ions such as Na^+ or Li^+ (Maier, 1999). In addition, α-quartz is usually twinned, with the possibility that twin walls enhance or reduce ionic diffusivity. Calleja *et al.* (2001) investigated transport within and perpendicular to Dauphiné twin walls. They found, using molecular dynamics simulation of ionic transport in an electric field, that the relaxed twin structure contains highly deformed channels inside the twin wall (Fig. 2). The wall thickness is ~1.3 nm, and the wall energy was estimated to be 9.5×10^{-2} Jm^{-2}. The minimum cross-sectional distances measured in the (001) plane are 0.32 nm in the bulk channels and much smaller (0.273 nm) in the wall channels. Transport along [001] is larger in the bulk crystal than in the domain walls, where the deformed channels act as bottlenecks for the diffusion. Quartz also exhibits channels along [110]. Calleja *et al.* (2001) found that overall conductivity along this direction is poorer than along [001], with a greater applied electric field necessary to promote inter-cavity motion. In this case transport is greater in the wall than in the bulk. This property can again be related to the greater circular cross-section of the conducting channel (this time of the wall channels rather than the bulk). Strong trapping of ions in the walls was

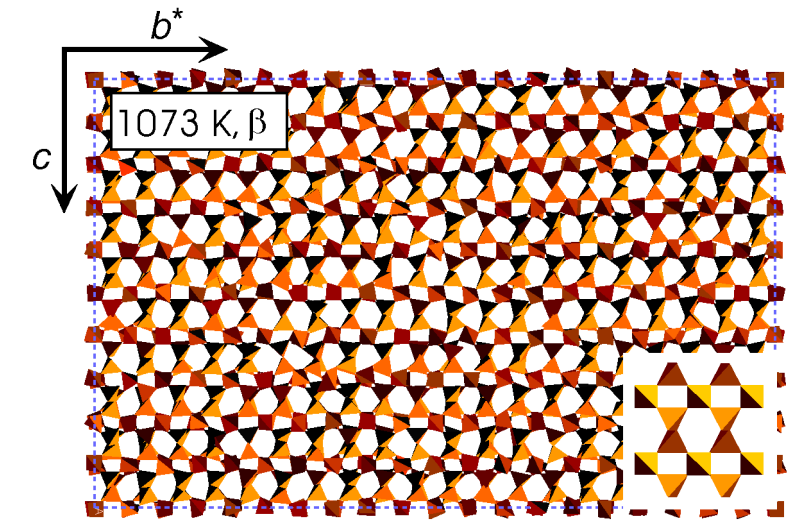

FIG. 1. (100) layers of instantaneous Reverse Monte Carlo atomic configurations in quartz. The insert shows the 'average' structure obtained from the configuration (Tucker *et al.*, 2000).

found for transport along [100]; unpinning energies for Na^+ and Li^+ were calculated for the various scenarios.

This is the first study to demonstrate that highly anisotropic ionic transport in a mineral is not only influenced by structural features in the bulk

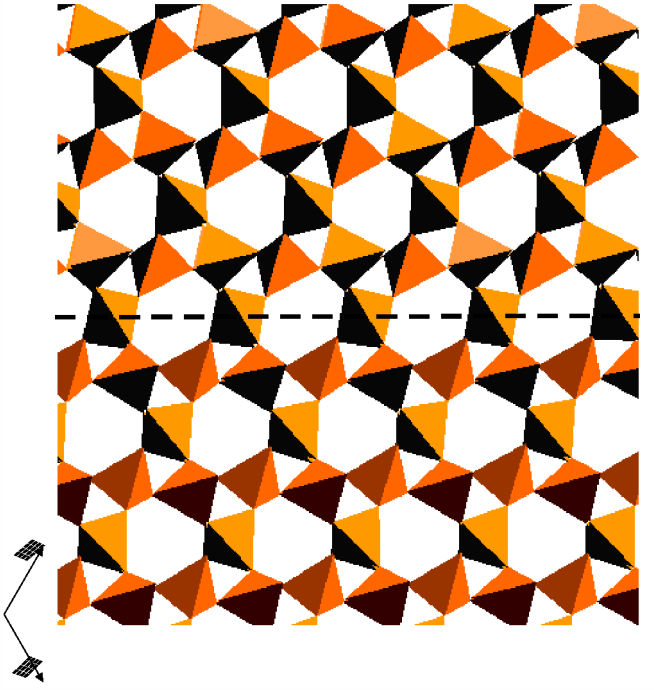

FIG. 2. The domain wall in quartz (dashed line) at T = 10 K viewed along [001] (Calleja *et al.*, 2001). Note the distorted channels within the wall.

structure but also, in a complex manner, by structural relaxations inside twin walls. Experimental work on twin walls in WO_3 has shown that both Na diffusion into the crystal and O diffusion out of the crystal are made faster along twin walls than in the bulk. Aird and Salje (1998, 2000) succeeded in doping twin walls to an average composition of $Na_{0.13}WO_3$ while the contamination of the bulk with Na was <3%. The high Na content of the walls is due to higher Na mobility in the walls. Dopants move firstly along the walls, then spread sideways through the bulk.

While the enhanced wall transport can be directly observed in WO_3 and reduced wall transport along [001] can be simulated in quartz, the situation is much harder to analyse in feldspars with very low mobility of Si and Al. Camara *et al.* (2000) examined anorthoclase ($(Na,K)AlSi_3O_8$) that contained minor amounts of Ca dissolved via the substitution

$$Na, K + Si = Ca + Al$$

Twin formation occurs via several structural phase transitions (Smith and Brown, 1988; Brown and Parsons, 1994) with the relevant transition $C2/m - C\bar{1}$ being displacive and of second order (Salje, 1985; Salje *et al.*, 1985). Twinning also occurs by ordering Si and Al. The time evolution of the latter was simulated by Tsatskis and Salje (1996) while the displacive twinning was studied in detail by Hayward and Salje (1996, 2000). These authors reported that the memory effect of twinning disappears after prolonged heating at temperatures at and above 880 K (twin amnesia) while memory remains preserved at lower temperatures. The possibility was discussed that the temperature of 880 K may be indicative of the solvus temperature of this anorthoclase (Or_{25}) (Smith and Brown, 1988) so that segregation of Na and K may be related to pinning via the enrichment on twin walls. Subsequent careful investigations of Camara *et al.* (2000) using analytical transmission electron microscopy (ATEM) found a weak increase of the K/Na ratio near twin walls, while the walls are also enriched in alkali and depleted in Ca and Al. This study reinforces the observation that twin walls not only show significant structural variations as compared with the bulk structure but also often possess different chemical compositions.

The $\alpha-\beta$ transition in agate

Two characteristic effects of nanomaterials are the importance of surface relaxations and boundary conditions. Pertsev and Salje (2000) developed a theory of the effect of elastic clamping on ferroelastic phase transitions. In this approach a thermodynamic potential is derived in which minima correspond to equilibrium thermodynamic states of an ellipsoidal ferroelastic inclusion surrounded by a linear elastic matrix. Strong bilinear coupling between the order parameter and strain leads to shifts of the transition temperature due to the mechanical inclusion/matrix interaction. Clamping by the matrix may also change the order of the transition and introduce the formation of new phases. Numerical estimates for the coelastic $\alpha-\beta$ transition in quartz (Pertsev and Salje, 2000) lead to the prediction that fully compacted nanoquartz should undergo a second-order phase transition rather than the strongly first-order transition of free-standing single crystals. Ríos *et al.* (2001) investigated the transition in agates from various locations that contained only microcrystalline quartz but there were no visible amounts of moganite or other SiO_2 phases. The average grain-sizes varied between 60 and 90 nm.

Experimental data from XRD, DSC and SHG all showed that the stepwise transition in quartz becomes continuous in agate, in agreement with the theoretical prediction. In addition, excess entropy is also observed above the transition point. The tail is believed to originate from defect fields (e.g. hydrous species) and surface relaxations; a quantitative analysis is given by Ríos *et al.* (2001). This example demonstrates clearly that highly compacted, nanometer-sized cystals show thermodynamic properties that are significantly different from those of equivalent larger single crystals.

Surface relaxations in hydroxylapatite

A characteristic mesoscopic feature is the surface relaxation that leads to subtle structural changes over many layers beneath the surface. Surface relaxations in small crystallites show equally important effects to those due to compact boundary conditions. Lee *et al.* (1999) and Lee and Salje (2000) showed that surface relaxations can have a symmetry-breaking effect on growth morphologies, producing equilibrium platelet morphologies even when these are inconsistent with the symmetry of the crystal. They are also responsible for strong heterogeneities of diffusion coefficients for penetration of dopants through the surface (Novak and Salje, 1998*a*,*b*).

Atomic simulations of the hydroxylapatite structure by Lee and Salje (2000) and Lee *et al.* (2000) demonstrated that relaxation processes due to two opposite surfaces in a slab with two (100) free surfaces can lead to platelet or needle growth. Posner *et al.* (1984) reported, indeed, that when hydroxylapatite is grown from solution it grows with a needle morphology while platelet growth occurs under *in vivo* conditions.

Surface relaxations were found to fall into two categories. The first category of relaxations only occurs very close to the surface; these relaxations have the effect of reducing the surface energy of the system. The second category of relaxations penetrates some distance from the bulk. Not only do these relaxations reduce the surface energy, but they also provide an energy of interaction between opposite surfaces if the slab is not too thick. The surface relaxations strongly distort the polygons formed by the calcium ions surrounding the hydroxide channels adjacent to the surface. Simultaneously the tetrahedral phosphate ions are distorted near the surface (Lee and Salje, 2000; Lee *et al.*, 2000). The degree of distortion is quantified by the standard deviation of P–O bond length within the phosphate tetrahedron. The degree of distortion increases significantly from the bulk values only for tetrahedral phosphate ions in unit cells immediately adjacent to the surface.

The second quantitative measure of distortion of the phosphate ions is their internal dipole moment measured in units of eÅ where e is the magnitude of the electron charge. The dipole of the tetrahedral phosphate is perpendicular to the surface for a system ten layers of unit cells thick. It is seen that the polarization persists for a few unit-cell distances into the bulk. The relaxation is oscillatory and contributes to the surface energy (Fig. 3). In summary, surface relaxations are relevant for growth morphologies and contribute significantly to the surface energy. Furthermore the structural states close to the surface can be significantly different from those of the bulk material. In this respect, surface relaxations are similar to twin walls.

While most work on surface relaxations and twin walls is based on atomic simulations of discrete structures, an equivalent continuum elasticity approach was recently developed by Conti and Salje (2001). While this approach leads to the same principle features as atomistic models, it requires substantially less computer power and allows us to explore physically meaningful parameter space more easily. These authors also derive an analytical solution for the interaction between twin walls and surface relaxation which shows zones of soft elastic responses at the intersection between twin walls and surfaces.

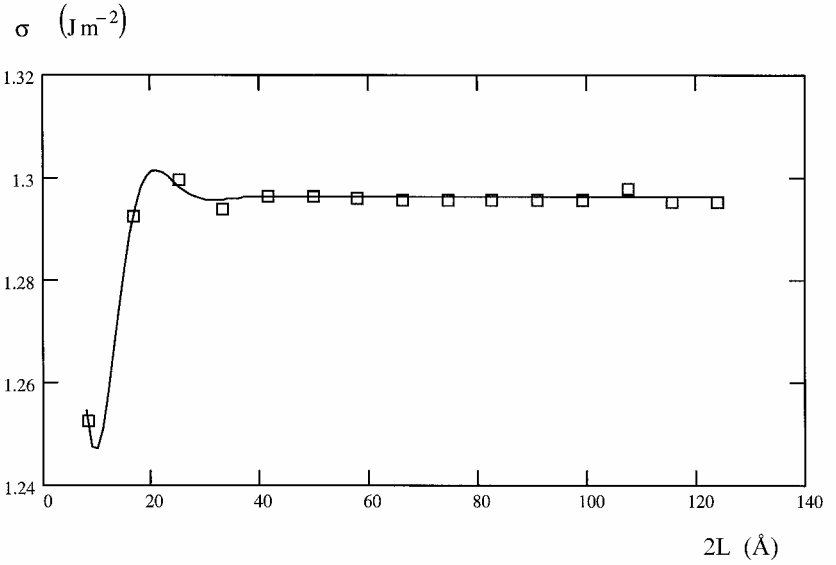

FIG. 3. Surface energy of a (100) surface as a function of the distance from an opposite (100) surface in hydroxylapatite (Lee *et al.*, 2000). L is half of the distance separating the surfaces.

Topological walls and sandwich domains in cordierite

Non-interacting twin walls in minerals tend to be aligned along elastically soft directions so that the elastic strain tensors in the adjacent domains are compatible without the formation of secondary strain fields (Salje, 1993; Sapriel, 1975; Fousek and Janovek, 1969). These walls are straight and clearly defined with little deviation from the soft direction unless additional interactions with defects, other domain walls, surfaces etc., occur (Salje and Ishibashi, 1996; Salje *et al.*, 1998*b*). Blackburn and Salje (1999*a,b,c*) noticed that exceptions to this rule exist if the elastic constraints are weak, e.g. in cases of materials with very small spontaneous strain. Cordierite is such an example. This mineral shows a very complex, patchy microstructure with poorly defined, wiggly domain walls and blunt needle domains (Venkatesh, 1954; Müller and Schreyer, 1991). Although there is a tendency for walls to align along soft directions, this appears to be much weaker than in other ferroelastics and some walls are observed which are not along elastically soft directions. Blackburn and Salje (1999*a*) undertook atomistic simulations of the phase transition in cordierite and found that two mechanisms compete for the formation of twin walls. The first mechanism is related to non-local elastic interactions as is characteristic for ferroelastics. The second mechanism involves only local topological interactions.

The essential ordering mechanism in cordierite relates to the rotation of six-member rings that contain two Al on opposite sides of the ring and four Si, two of which are between each pair of Al (Fig. 4). Tetrahedra containing Al are slightly larger than those containing Si, and this leads to a deformation of the rings. If we now allocate a pseudo-spin in the direction connecting two Al positions in a ring, we find that 3 pseudo-spin positions are possible. In using this nomenclature we reduce the system to a three-state Potts-model

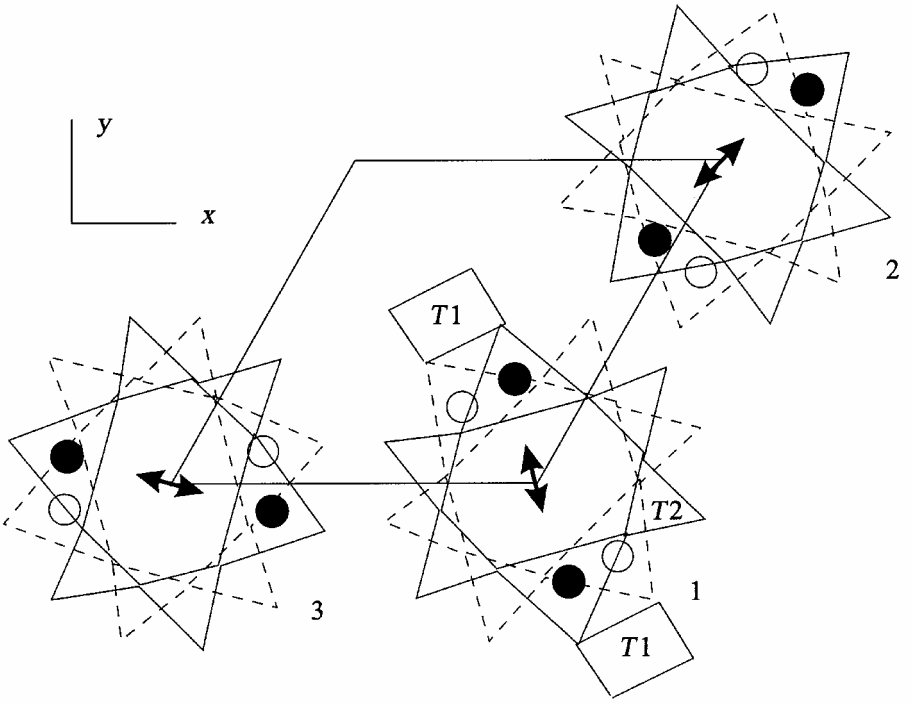

FIG. 4. Schematic representation of the cordierite structure (Blackburn and Salje, 1999*a*). *T*1/*T*2 indicate the two types of oxygen tetrahedra present in the structure, with Al atoms (black and white circles) and Si atoms in their centres. Numbers (1,2,3) indicate the three possible configurations of the Al pair, which can be described by an arrow such as the one shown in the centre of the ring. The *x*-*y* axes correspond to the orthorhombic domain with the Al pair in configuration 1.

in 3D (Eichhorn and Binder, 1996; Binder, 1981). The orientation of topological walls and strain walls follows then from the relationship between the pseudo-spin in adjacent domains (Fig. 5) and represent non-global energy minima of the system.

Blackburn and Salje (1999*c*) argued that strain walls and topological walls can combine to produce a novel wetting phenomenon. In Fig. 6 such a 'sandwich' domain configuration is shown. The two outer domains would form a strain wall if directly connected but contain a slice of the third domain type in between. The actual domain interfaces are topological in nature while the global configuration relates to a classic strain minimization. Extensive molecular dynamics simulations have shown that, at least on a scale of several unit cells, such sandwich configurations occur at temperatures well below the transition point (Blackburn and Salje, 1999*c*).

Microstructure of radiation-damaged minerals

The microstructure resulting from the amorphization process in radiation-damaged minerals is complex and strongly governs the chemical and physical properties of minerals. Leaching rates, for example, increase by one to two orders of magnitude, and this renders the phenomenon very important when dealing with synthetic analogues for nuclear waste disposal (Weber *et al.*, 1998). If actinides are meant to be confined inside a matrix, it has to remain resistant, at least in part, to internal radiation damage.

Amorphization originates as a consequence of the α-decay of the radioactive impurities contained in these minerals (Holland and Gottfried, 1955). Heavy recoil nuclei (100 keV) created during the decay process undergo ballistic collisions with the atoms of the surrounding

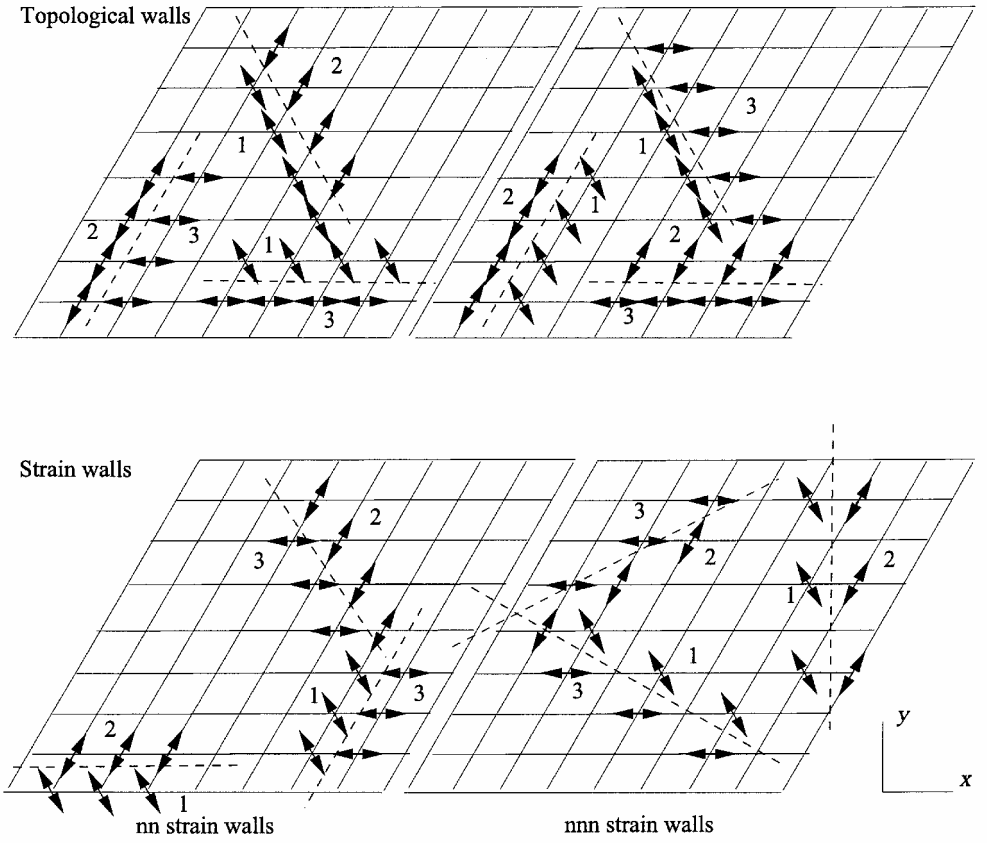

FIG. 5. Strain and topological walls (dashed lines) obtained in a computer simulation for cordierite (Blackburn and Salje, 1999*a*). Arrows indicate the alignment of the pseudo-spin describing the position of the Al pairs within the ring. The actual Al positions shown in Fig. 4 are rotated by ±15° with respect to the arrow direction.

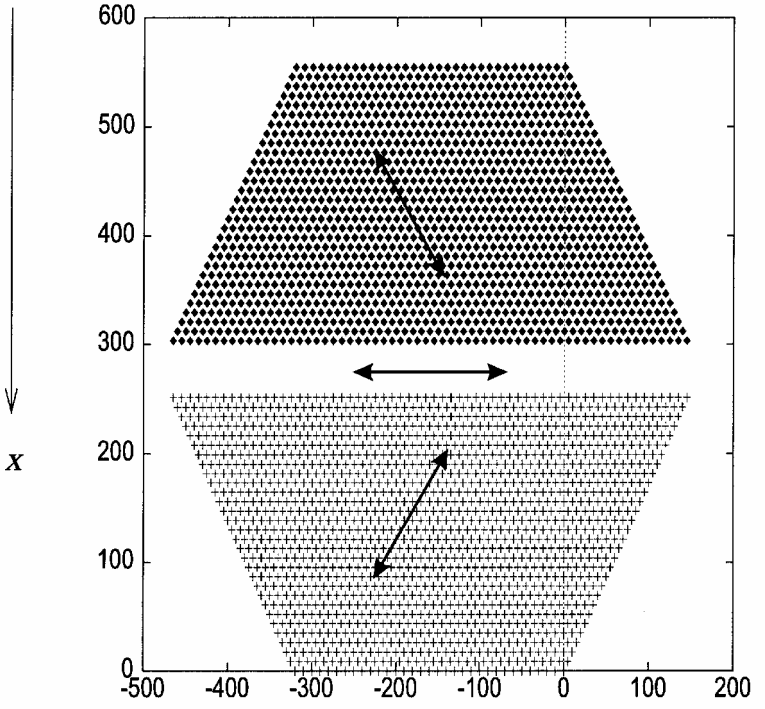

FIG. 6. Sandwich-type wall in cordierite (Blackburn and Salje, 1999*a*). Arrows describe the three different orientations of the pseudo-spin.

crystalline matrix disrupting locally the long-range order of the structure. For sufficiently high damage-accumulation, the system becomes amorphous (Weber *et al.,* 1994). The crystalline to amorphous transformation is thus related to the percolation of either amorphous cascades or crystalline islands. At each of the percolation points the minority state ceases to be "island in a matrix" (Salje *et al*., 1999).

Zircon as a model

Given the relatively simple structure and the large amount of experimental data available, zircon is regarded as a model mineral for understanding the structural changes involved during radiation damage. Within an α-dose range of 10^{18}–10^{19} α-decay events/g, natural zircon undergoes amorphization, with a bulk modulus decrease of ~60%, and a volume increase of 18% (Ewing, 1999). Surprisingly this gives rise to hardly any crack creation in unzoned specimens, but when heterogeneous uranium distributions are present, the heterogeneous volume swelling may lead to cracking.

Systems such as zircon could, as a first approach, be interpreted in terms of a two-phase system: (1) the original crystalline matrix; and (2) the amorphous regions produced by recoil nuclei. Nevertheless, this simplification has recently been shown to be inadequate as the structural properties of the two phases involved (crystalline/amorphous) evolve gradually in order to accommodate further damage accumulation.

Damage accumulation

The mechanism of amorphization for a given system depends on the nature of the radiation damage – whether by α-decay, heavy ions, neutron irradiation, etc. (Wang *et al.,* 2000) – and on the crystalline structure of the system. Zircons with large uranium contents are mostly found in an amorphous state, whereas monazite ($CePO_4$), for example, is almost invariably in a crystalline state (Meldrum *et al.,* 1996). The fraction of amorphous material created as a function of the degree of damage (or dose) is a suitable parameter for determining the mechanism of amorphization. The steep increase at low doses (Fig. 7) observed by independent experimental

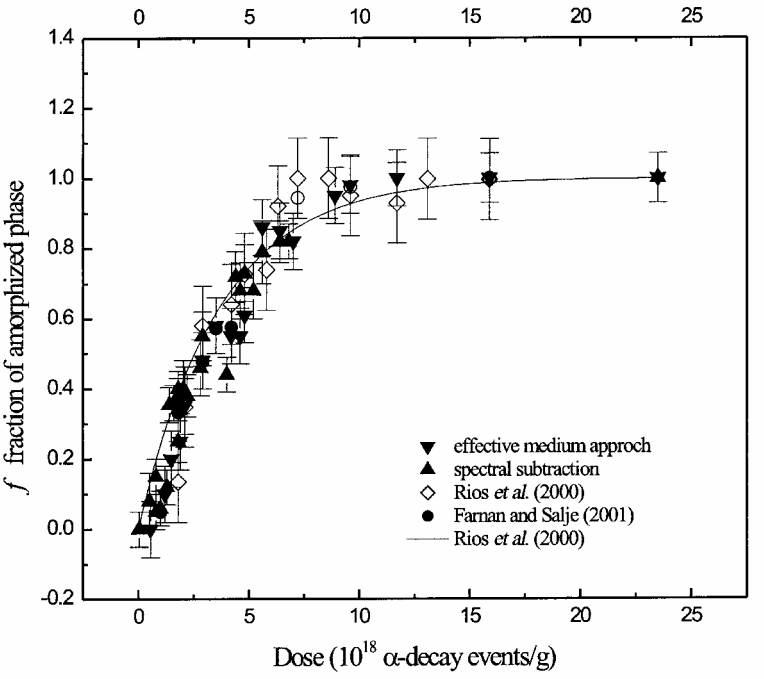

FIG. 7. Fraction of amorphous material as a function of radiation dose obtained in zircon by X-rays, Si-NMR and infrared spectroscopy (Zhang and Salje, 2001).

techniques (X-rays (Ríos *et al*., 2000*a*), Si-NMR (Farnan and Salje, 2001) and infrared spectroscopy (Zhang and Salje, 2001)) indicates that amorphous material is produced within the amorphous cascade, following the direct impact of the recoil nucleus. In the case of zircon, the structure is not able to recover, or at least not totally, after the impact, which therefore leaves a highly disordered region of ~5 nm diameter. As damage is accumulated, more of these displacement cascades are generated. On average, some 3000 atoms are displaced per α-recoil nucleus (Farnan and Salje, 2001).

Nature of the structural changes during amorphization

During amorphization, the crystalline matrix expands (by up to 1.5% along *a* and 2.5% along *c*) in order to accommodate the interstitials/vacancies produced by the α-particles generated together with the recoil nuclei (Murakami *et al.,* 1991). The anisotropic character of the expansion – larger along *c* than *a* – is due to a preferential defect recovery across the basal plane. In zircon, strong ZrO_8–SiO_4–ZrO_8 edge-sharing linkages exist along the tetragonal *c* axis, making it difficult for the structure to relax when accommodating defects. On the contrary, the recovery across the basal plane is favoured by the weaker linkages between corner-sharing ZrO_8–ZrO_8 units. These latter bonds allow a certain degree of freedom in such a way that ZrO_8 units can twist with respect to each other (within the basal plane) allowing the structure to relax (Ríos *et al.,* 2000*b*). This deformation is believed to be at the origin of the shear waves observed by X-ray diffuse scattering (Ríos and Salje, 1999). Recent molecular dynamics simulations (Trachenko *et al.,* 2002) suggest that part of the shear deformation could also be related to the cascade formation itself.

The anisotropic behaviour of the damage accumulation is also reflected during the recovery of the structure after thermal annealing. At temperatures of ~1000 K, defects across the basal plane have mostly annealed. Only at temperatures as high as 1300 K do the defects along the *c* axis start to anneal (Geisler, 2002). This anisotropic behaviour can be related to two important aspects of the structure of zircon: firstly, to the anisotropy of the type of linkages present in zircon and described above (corner *vs.* edge-sharing) and, secondly, to the structure of

the ZrO_8 polyhedron itself, which comprises two oxygen shells, one close (~0.213 nm) and one far (~0.228 nm) from the central Zr atom. This arrangement permits the ZrO_8 unit to have independent behaviour along the *a* and *c* axes, respectively.

Recent research has particularly focused on the structural aspects of the glassy phase. Even though the actual structure remains unsolved, indirect evidence from X-ray diffraction (Ríos *et al.,* 2000*a*) indicates that the amorphous phase produced during radiation damage is not topologically unique, but depends on the actual degree of damage accumulation. Experimental evidence for such a structural rearrangement as a function of the α-dose has only been observed recently by Si-NMR (Farnan and Salje, 2001) and amorphous cascade modelling (Trachenko *et al.,* 2001; Crocombette and Ghaleb, 2001). In these papers, gradual polymerization of SiO_4 species (isolated in the crystalline structure) was shown to occur inside the amorphous cascades with increasing cumulative α-dose. This means that the structure of amorphous regions evolves gradually as the number of ballistic impacts increases, in the same way as the structure of the crystalline phase rearranges itself in order to accommodate α-particle-induced defects. Moreover, amorphous cascades produced during simulations (with 30–70 keV recoil nuclei) have been found, surprisingly, to be inhomogeneous, showing a densified rim surrounding a low-density cavity in the core (Trachenko *et al.,* 2002). This is an effect that does not show in the simulations when the recoil nucleus has smaller energies, ~10 keV (Crocombette and Ghaleb, 2001). The densified rim is populated with polymerized SiO_4 units. As amorphous cascades start to overlap, more densified rims and depleted regions are produced, leading to a higher degree of polymerization. The enormous volume swelling observed in zircon might therefore be a consequence of the large cavities produced during cascade production and subsequent accumulation.

Acknowledgements

One of the authors (SR) thanks NERC for financial support.

References

Aird, A. and Salje, E.K.H. (1998) Sheet superconductivity in twin walls: experimental evidence of WO_{3-x}. *Journal of Physics: Condensed Matter,* **10,** L377–L380.

Aird, A. and Salje, E.K.H. (2000) Enhanced reactivity of domain walls in WO_3 with sodium. *The European Physical Journal B,* **15,** 205–210.

Axe, J.D. and Shirane, G. (1970) Study of the α-β quartz phase transformation by inelastic neutron scattering. *Physical Review B,* **1,** 342–348.

Binder, K. (1981) Static and dynamic critical phenomena of the two-dimensional Q-state Potts-model. *Journal of Statistical Physics*, **24**, 69–86.

Blackburn, J.F. and Salje, E.K.H. (1999*a*) Sandwich domain walls in cordierite: a computer simulation study. *Journal of Physics: Condensed Matter,* **11,** 4747–4766.

Blackburn, J.F. and Salje, E.K.H. (1999*b*) Time evolution of twin domains in cordierite: a computer simulation study. *Physics and Chemistry of Minerals,* **26,** 275–296.

Blackburn, J.F. and Salje, E.K.H. (1999*c*) Formation of needle shaped twin domains in cordierite: a computer simulation study. *Journal of Applied Physics,* **85,** 2414–2422.

Brown, W.L. and Parsons, I. (1994) Feldspars in igneous rocks. Pp. 449–500 in: *Feldspars and their Reactions* (I. Parsons, editor). Kluwer Academic Publishers, Dordrecht, The Netherlands.

Calleja, M., Dove, M.T. and Salje, E.K.H. (2001) Anisotropic ionic transport in quartz: the effect of twin boundaries. *Journal of Physics: Condensed Matter,* **13**, 9445–9454.

Camara, F., Doukhan, J.C. and Salje, E.K.H. (2000) Twin walls in anorthoclase are enriched in alkali and depleted in Ca and Al. *Phase Transitions,* **71**, 227–242.

Carpenter, M.A. and Salje, E.K.H. (1994*a*) Thermodynamics of non-convergent cation ordering in minerals, II: spinels and the orthopyroxene solid solution. *American Mineralogist,* **79**, 1068–1083.

Carpenter, M.A. and Salje, E.K.H. (1994*b*) Thermodynamics of non-convergent cation order in minerals, III: order parameter coupling in potassium feldspar. *American Mineralogist,* **79**, 1084–1098.

Carpenter, M.A. and Salje, E.K.H. (1998) Elastic anomalies in minerals due to structural phase transitions. *European Journal of Mineralogy,* **10**, 693–812.

Carpenter, M.A., Salje, E.K.H. and Graeme-Barber, A. (1998*a*) Spontaneous strain as a determinant of thermodynamic properties for phase transitions in minerals. *European Journal of Mineralogy,* **10**, 621–691.

Carpenter, M.A., Salje, E.K.H., Graeme-Barber, A., Wruck, B., Dove, M.T. and Knight S.K. (1998*b*) Calibration of excess thermodynamic properties and elastic constant variations associated with the α↔β

phase transition in quartz. *American Mineralogist,* **83**, 2–22.

Conti, S. and Salje E.K.H. (2001) Surface structure of ferroelastic domain walls: a continuum elasticity approach. *Journal of Physics: Condensed Matter,* **13**, L847–L854.

Crocombette, J.P. and Ghaleb, D. (2001) Molecular dynamics modelling of irradiation damage in pure and uranium-doped zircon. *Journal of Nuclear Materials*, **295**, 167–178.

Eichhorn, K. and Binder K. (1996) Monte Carlo investigation of the three-dimensional random-field three-state Potts-model. *Journal of Physics: Condensed Matter,* **8**, 5209–5227.

Ewing, R.C. (1999) Nuclear waste forms for actinides. *Proceedings of the National Academy of Science USA*, **96**, 3432–3439.

Farnan, I. and Salje, E.K.H. (2001) The degree and nature of radiation-damage in zircon observed by ^{29}Si nuclear magnetic resonance. *Journal of Applied Physics,* **89**, 2084–2090.

Fousek, J. and Janovek, V. (1969) The orientation of domain walls in twinned ferroelectric crystals. *Journal of Applied Physics*, **40**, 135–142.

Geisler, T. (2002) Isothermal annealing of partially metamict zircon: evidence for a three-stage recovery process. *Physics and Chemistry of Minerals*, **29**, 420–429.

Hayward, S.A. and Salje, E.K.H. (1996) Displacive phase transition in anorthoclase: The "plateau effect" and the effect of T1–T2 ordering on the transition temperature. *American Mineralogist,* **81**, 1332–1336.

Hayward, S.A. and Salje, E.K.H. (1999) Cubic-Tetragonal phase transition in $SrTiO_3$ revisited: Landau theory and transition mechanism. *Phase Transitions,* **68,** 501–522.

Hayward, S.A. and Salje, E.K.H. (2000) Twin memory and twin amnesia in anorthoclase. *Mineralogical Magazine,* **64**, 195–200.

Holland, H.D. and Gottfried, D. (1955) The effect of nuclear radiation on the structure of zircon. *Acta Crystallographica,* **8**, 291–300.

Lee, W.T., Salje, E.K.H. and Dove, M.T. (1999) Effect of surface relaxations of the equilibrium growth morphology of crystals: platelet formation. *Journal of Physics: Condensed Matter,* **11,** 7385–7410.

Lee, W.T. and Salje, E.K.H. (2000) Oscillatory zoning caused by oscillating surface relaxations. *The European Physical Journal B*, **13**, 395–398.

Lee, W.T., Dove, M.T. and Salje, E.K.H. (2000) Surface relaxations in hydroxyapatite. *Journal of Physics: Condensed Matter,* **12**, 9829–9841.

Maier, J. (1999) Grain boundary effects in ionic and mixed conductors. *Solid Sate Phenomena,* **67–8**, 45–54.

Malcherek, T., Kroll, H., Schleiter, M. and Salje, E.K.H. (1995) The kinetics of the monoclinic to monoclinic phase transition in $BaAl_2Ge_2O_8$-feldspar. *Phase Transitions,* **55**, 199–215.

Malcherek, T., Salje, E.K.H. and Kroll, H. (1997) A phenomenological approach to ordering kinetics and partially conserved order parameters. *Journal of Physics: Condensed Matter,* **9**, 8075–8084.

Meldrum, A., Wang, L.M. and Ewing, R.C. (1996) Ion beam induced amorphization of monazite. *Nuclear Instruments and Methods in Physics Research B,* **116**, 220–224.

Müller, W.F. and Schreyer, W. (1991) Microstructural variations in a natural cordierite from the Eifel volcanic field, Germany. *European Journal of Mineralogy,* **3**, 915–931.

Murakami, T., Chakoumakos, B.C., Ewing, R.C., Lumpkin, G.R. and Weber, W.J. (1991) Alpha-decay event damage in zircon. *American Mineralogist,* **76,** 1510–1532.

Müser, M.H. and Binder, K. (2001) Molecular dynamics study of the α-β transition in quartz: elastic properties, finite size effects, and hysteresis in the local structure. *Physics and Chemistry of Minerals,* **28,** 746–755.

Novak, J. and Salje, E.K.H. (1998*a*) Surface structure of domain walls. *Journal of Physics: Condensed Matter,* **10**, L359–L366.

Novak, J. and Salje, E.K.H. (1998*b*) Simulated mesoscopic structures of a domain wall in a ferroelastic lattice. *The European Physical Journal B*, **4**, 279–284.

Ordejón, P., Artacho, E. and Soler, J.M. (1996) Self-consistent order-N density-functional calculations for very large systems. *Physical Review B,* **53**, 10441–10444.

Pérez-Mato, J.M. and Salje, E.K.H. (2001) Order parameter saturation at low temperatures: displacive phase transitions with coupled Einstein oscillators. *Philosophical Magazine Letters,* **81**, 885–891.

Pertsev, N.A. and Salje, E.K.H. (2001) Thermodynamics of pseudo-proper and improper ferroelastic inclusions and polycrystals: Effect of elastic clamping on phase transitions. *Physical Review B,* **61**, 902–908.

Posner, A.S., Blumenthal, N.C. and Betts, F. (1984) *Chemistry and Structure of Precipitated Hydroxyapatite in Phosphate Minerals* (J.O. Nriagju and P.B. Moore, editors), Springer, New York.

Ríos, S. and Salje, E.K.H. (1999) Diffuse X-ray scattering from weakly metamict zircon. *Journal of Physics: Condensed Matter,* **11**, 8947–8956.

Ríos, S., Salje, E.K.H., Zhang, M. and Ewing, R.C. (2000*a*) Amorphization in zircon: evidence for direct impact damage. *Journal of Physics: Condensed Matter,* **12**, 2401–2412.

Ríos, S., Malcherek, T., Salje, E.K.H. and Domeneghetti, C. (2000*b*) Localized defects in radiation-damaged zircon. *Acta Crystallographica B,* **56**, 947–952.

Ríos, S., Salje, E.K.H. and Redfern, S.A.T. (2001) Nanoquartz vs. macroquartz: a study of the alpha-beta phase transition. *The European Physical Journal B,* **20**, 75–83.

Salje, E.K.H. (1985) Thermodynamics of sodium feldspar I: order parameter treatment and strain induced coupling effects. *Physics and Chemistry of Minerals,* **12**, 93–98.

Salje, E.K.H. (1992*a*) Application of Landau theory for the analysis of phase transitions in minerals. *Physics Reports,* **215**, no.2, 49–99.

Salje, E.K.H. (1992*b*) Phase transitions in minerals: from equilibrium properties towards kinetic behaviour. *Berichte der Bunsen-Gesellschaft für physikalische Chemie no.* **11**, 1518–1541.

Salje, E.K.H. (1993) *Phase Transitions in Ferroelastic and Co-elastic Crystals* (student edition). Cambridge University Press, Cambridge, England, 276 pp.

Salje, E.K.H. (1994) Phase transitions and vibrational spectroscopy in feldspars. Pp. 103–160 in: *Feldspars and Their Reactions* (I. Parsons, editor). NATO ASI series. Kluwer Academic Publishers, Dordrecht, The Netherlands.

Salje, E.K.H and Ishibashi, Y. (1996) Mesoscopic structures in ferroelastic crystals: needle twins and right-angled domains. *Journal of Physics: Condensed Matter,* **8**, 8477–8495.

Salje, E.K.H., Kuscholke, B., Wruck, B. and Kroll, H. (1985) Thermodynamics of sodium feldspar II: experimental results and numerical calculations. *Physics and Chemistry of Minerals,* **12**, 99–107.

Salje, E.K.H. Ridgwell, A., Güttler, B., Wruck, B., Dove, M.T. and Dolino, G. (1992) On the displacive character of the phase transition in quartz: a hard mode spectroscopy study. *Journal of Physics: Condensed Matter,* **4**, 571–577.

Salje, E.K.H., Gallardo, M.C, Jiménez Romero, F.J. and del Cerro, J. (1998*a*) The cubic-tetragonal phase transition in Strontium titanate: excess specific heat measurements and evidence for a near-tricritical, mean field type transition mechanism. *Journal of Physics: Condensed Matter,* **10,** 5535–5543.

Salje, E.K.H., Buckley, A., Van Tendeloo, G. and Ishibashi Y. (1998*b*) Needle twins and right-angled twins in minerals: comparison between experiment and theory. *American Mineralogist,* **83**, 811–822.

Salje, E.K.H., Chrosch, J. and Ewing, R.C. (1999) Is 'metamictization' of zircon a phase transition? *American Mineralogist,* **84**, 1107–1116.

Sapriel, J. (1975) Domain wall orientations in ferroelastics. *Physical Review B,* **12**, 5128–5140.

Smith, J.V. and Brown W.L. (1988) Crystal Structures, Physical Chemical and Microstructural Properties. In *Feldspar Minerals* **1** (2nd edition). Springer-Verlag, New York.

Tezuka, Y., Shin, S. and Ishigame, M. (1991) Observation of the silent soft phonon in β quartz by means of hyper-Raman Scattering. *Physical Review Letters,* **66**, 2356–2359.

Trachenko, K.O., Dove, M.T. and Salje, E.K.H. (2001) Atomistic modelling of radiation damage in zircon. *Journal of Physics: Condensed Matter,* **13**, 1947–1959.

Trachenko, K.O., Dove, M.T. and Salje, E.K.H. (2002) Structural changes in zircon under α-decay irradiation. *Physical Review B,* **65**, 180102(R)1–3.

Tsatskis, I. and Salje, E.K.H. (1996) Time evolution of pericline twin domains in alkali feldspars: a computer-simulation study. *American Mineralogist,* **81**, 800–810.

Tsuneyuki, S., Aoki, H. and Tsukada, M. (1990) Molecular-dynamics study of the α-structural to β-structural phase transition of quartz. *Physical Review Letters,* **64**, 776–779.

Tucker, M.G., Dove, M.T. and Keen, D.A. (2000) Simultaneous analysis of changes in long-range and short-range structural order at the displacive phase transition in quartz. *Journal of Physics: Condensed Matter,* **12**, L723–L730.

Venkatesh, V. (1954) Twinning in cordierite. *American Mineralogist,* **39**, 636–646.

Wang, S.X., Wang, L.M. and Ewing R.C. (2001) Irradiation-induced amorphization: effects of temperature, ion mass, cascade size, and dose rate. *Physical Review B,* **63**, 24105–24108.

Weber, W.J., Ewing, R.C. and Wang L.M. (1994) The radiation-induced crystalline to amorphous transition in zircon. *Journal of Materials Research,* **9**, 688–698.

Weber, W.J., Ewing, R.C., Catlow, C.R.A., Díaz de la Rubia, T., Hobbs, L.W., Kinoshita, C., Matzke, H., Motta, A.T., Nastasi, M., Salje, E.K.H., Vance, E.R. and Zinkle, S.J. (1998) Radiation effects in crystalline ceramics for the immobilization of high-level nuclear waste and plutonium. *Journal of Materials Research,* **13**, 1434–1484.

Zhang, M. and Salje, E.K.H. (2001) Infrared spectroscopic analysis in zircon: radiation damage and the metamict state. *Journal of Physics: Condensed Matter*, **13**, 3057–3071.

[*Manuscript received 23 January 2002*]